Supplementary figures

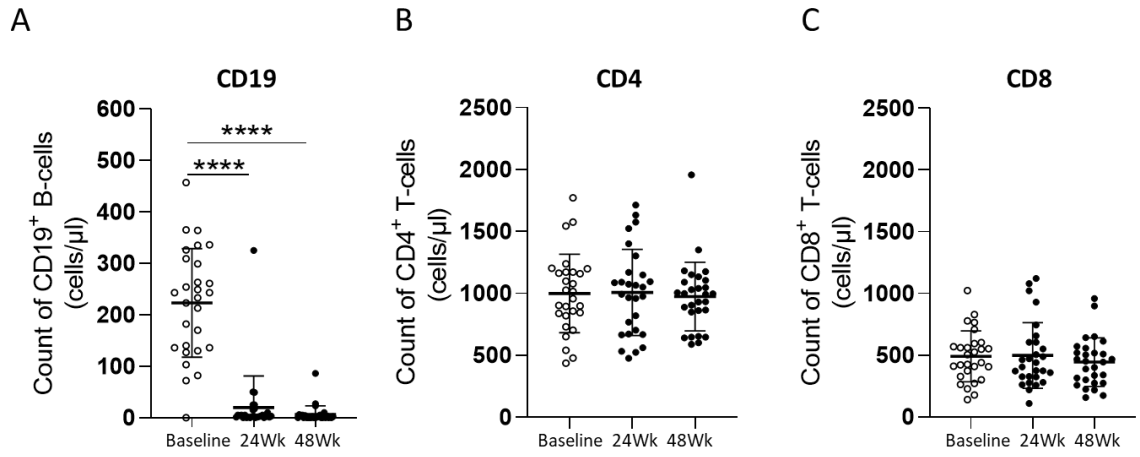

eFigure 1. Count of CD19$^+$ B-cells, CD4$^+$ and CD8$^+$ T-cells before and after OCR

(A) Cell counts of CD19$^+$ B-cells) subset within lymphocytes at baseline (white), 24 weeks (24 Wk) and 48 weeks (48 Wk) of OCR treatment (black) (Baseline 223 ± 105 cells/µl, 48 Wk 6 ±17 cells/µL. **(B)** Cell counts (cells/µl) of CD4$^+$ T-cells at baseline (white), 24 and 48 Wk of OCR treatment (black) (Baseline 999 ± 316 cells/µl, 48 Wk 974 ± 277 cells/µL). **(C)** Cell counts (cells/µl) of CD8$^+$ T-cells at baseline (white), after 24 and 48 Wk of OCR treatment (black) (Baseline 491 ± 206 cells/µl, 48 Wk 444 ± 197 cells/µL). *The counts of cells were calculated with the frequency and the complete blood count at baseline, 24 and 48 Wk of OCR. One-way ANOVA with correction by Tukey's multiple comparison test was used. *P < 0.05, **P < 0.01, ***P < 0.001, ****P < 0.0001 (mean with SD) (n = 32).*

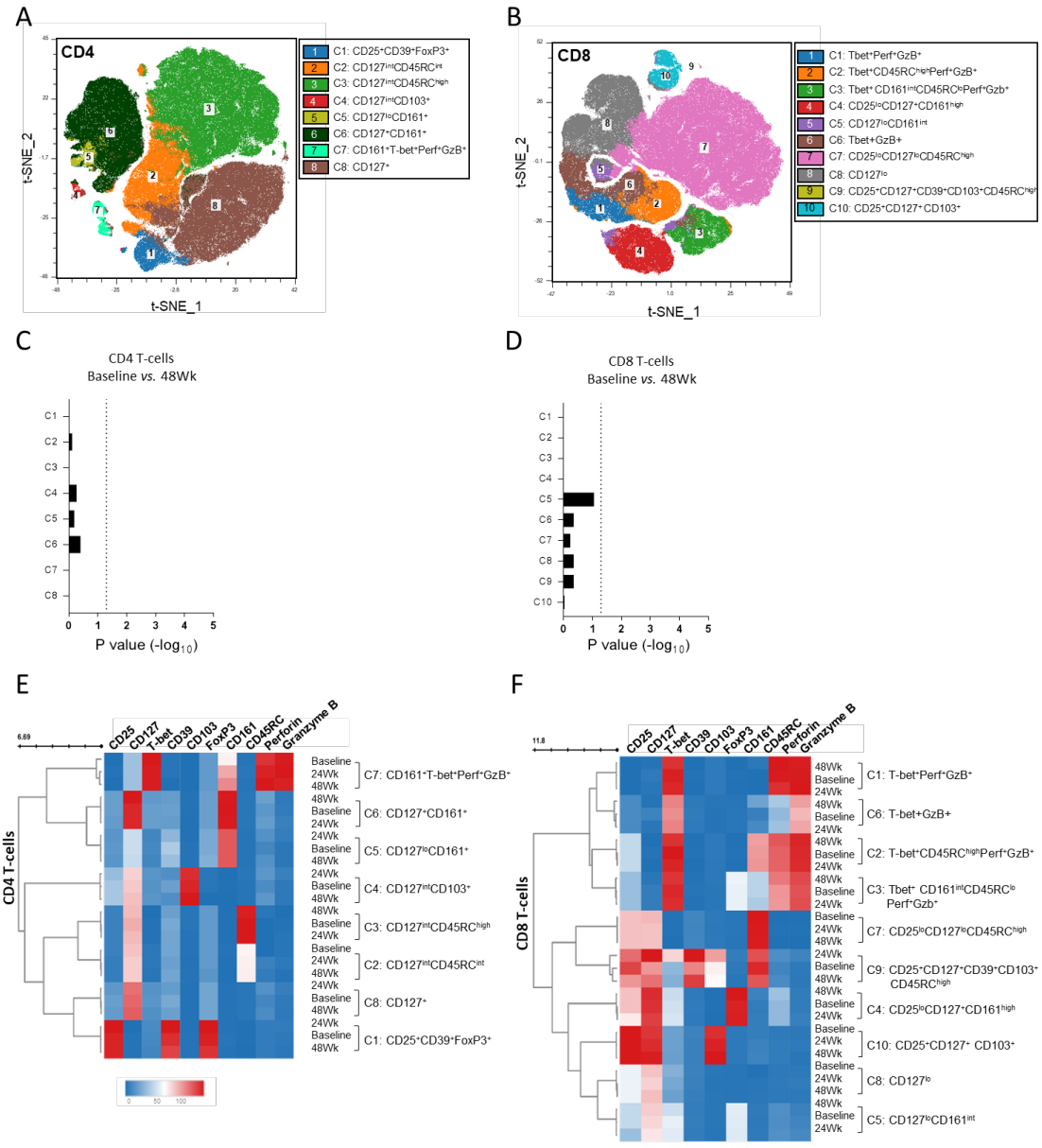

eFigure 2. No effect of ocrelizumab treatment on Treg subsets

(A-B) t-SNE CUDA projections of $CD4^+$ or $CD8^+$ T-cell clusters identified by FlowSOM meta-clustering ($1*10^4$ cells/patient/time point). **(C-D)** Representation of $CD4^+$ and $CD8^+$ T-cells adjusted P value to compare each cluster at baseline and after 48 Wk of OCR treatment. **(E-F)** Heatmap representation of the indicated markers for the $CD4^+$ and $CD8^+$ T-cell clusters at baseline, 24 and 48 Wk of OCR treatment. *Unsupervised analyses were performed on OMIQ (https://www.omiq.ai/) (A-B). The Bonferroni multiple test correction (C-D) was used. *P < 0.05, **P < 0.01, ***P < 0.001, ****P < 0.0001 (n = 32).*

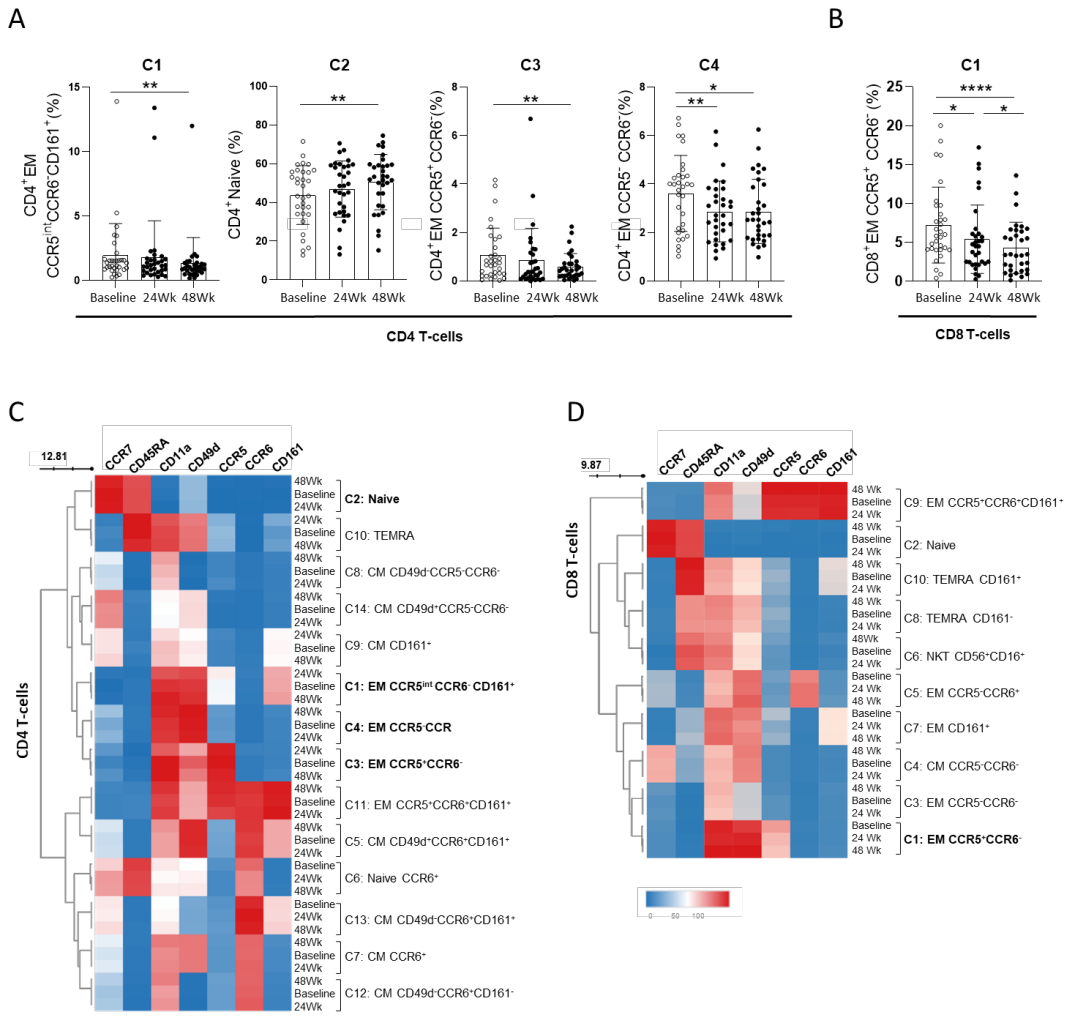

eFigure 3. Frequency and phenotype of CD4⁺ and CD8⁺ T-cell clusters modified by OCR

(A) Abundance of the **C1**, **C2**, **C3**, and **C4** clusters among the CD4⁺ T-cells at baseline, 24 and 48 Wk of OCR treatment (**C1**: Baseline 1.9 ± 2.4%, 48 Wk 1.3 ± -2%; **C2**: Baseline 43.9 ± 15.2%, 48 Wk 50.5 ± 14.3%; **C3**: Baseline 1.07 ± 1.1%, 48 Wk 0.59 ± 0.5% and **C4**: Baseline 3.6 ± 1.6%, 48 Wk 2.9 ± 1.3%). **(B)** Abundance of the C1 cluster among the CD8⁺ T-cells at baseline, 24 and 48 Wk of OCR treatment (Baseline 7.2 ± 4.9%, 48 Wk 4.2 ± 3.3%). **(C-D)** Heatmap representation of the indicated markers for the CD4⁺ and CD8⁺ T-cell clusters at baseline, 24 and 48 Wk of OCR. *One-way ANOVA with correction by Tukey's multiple comparisons (A-B) was used. *P < 0.05, **P < 0.01, ***P < 0.001, ****P < 0.0001 (mean with SD) (n = 32).*

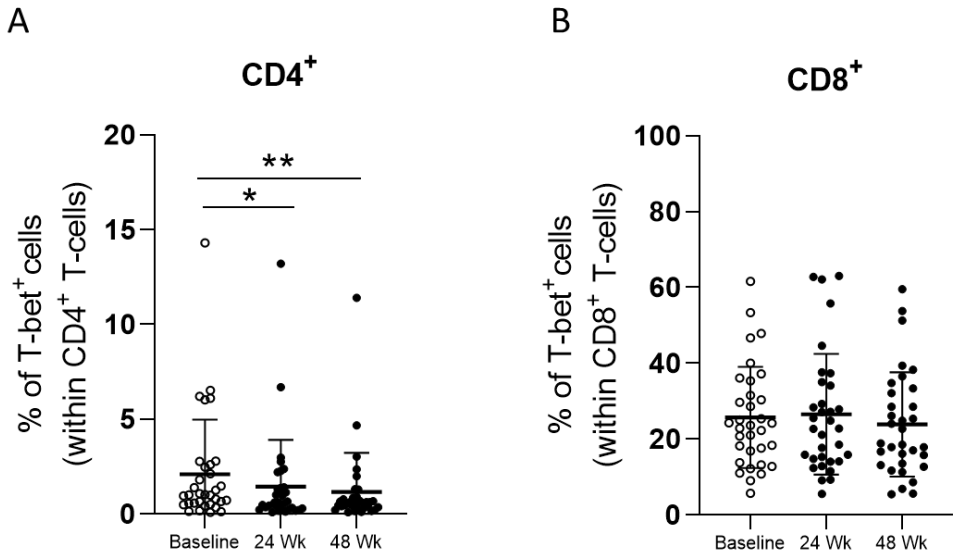

eFigure 4. Frequency of T-bet in CD4+ and CD8+ T-cells

Frequency of T-bet$^+$ cells among CD4$^+$ T-cells (Baseline 2.1 ± 2.9%, 48 Wk 1.2±2.1%) and CD8$^+$ T-cells (Baseline 25.7 ± 13.3%, 48 Wk 23.8±13.7%) subsets at baseline, 24 and 48 Wk of OCR treatment. *One-way ANOVA with correction by Tukey's multiple comparison test was used. *P < 0.05, **P < 0.01, ***P <0.001, ****P < 0.0001 (mean with SD) (n = 32).*

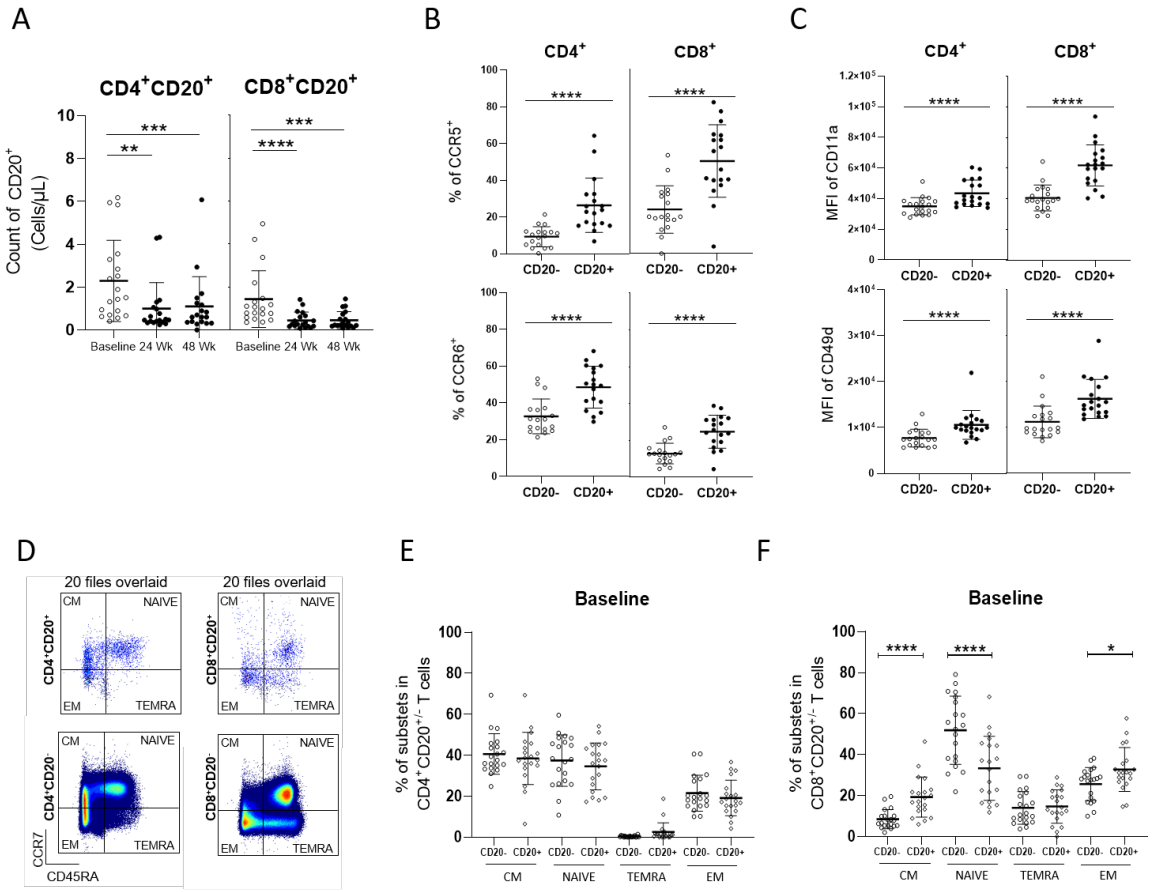

eFigure 5. Naive/memory subsets and phenotype of CD3$^+$CD20$^+$ T-cells.

(A) Cell counts (cells/µl) of CD4$^+$CD20$^+$ and CD8$^+$CD20$^+$ T-cells subset at baseline (white), 24 and 48 Wk of OCR treatment (black). **(B)** Frequency (%) of CCR5$^+$ and CCR6$^+$ cells within CD20$^-$ and CD20$^+$ cells at baseline. (**C**) Mean fluorescence intensity of CD11a and CD49d cells within CD20$^-$ and CD20$^+$ cells at baseline**. (D)** Gating strategy on 20 patients overlaid on CD4$^+$CD20$^{+/-}$ or CD4$^+$CD20$^{+/-}$ at baseline. The gating strategy is shown after the exclusion of dead cells and doublets. The CD4$^+$ and CD8$^+$ T-cells are analyzed with CD45RA and CCR7: naive (CD45RA$^+$CCR7$^+$), EM (CD45RA$^-$CCR7$^-$), CM (CD45RA$^-$CCR7$^+$), and TEMRA (CD45RA$^+$CCR7$^-$) cells. (**E**) Frequency of naive, TEMRA, EM, CM within CD4$^+$CD20$^+$ T-cells and CD4$^+$CD20$^-$ T-cells at baseline. (**F**) Frequency of naive, TEMRA, EM, CM within CD8$^+$CD20$^+$ and CD8$^+$CD20$^-$ T-cells at baseline. *The counts of cells were calculated with the frequency and the complete blood count at baseline 24 and 48 Wk* of OCR treatment. *Friedman test with Dunn's correction (A), paired t-test (B-C) and one-way ANOVA with correction by Greisser–Greenhouse (E-F) were used. *P < 0.05, **P < 0.01, ***P < 0.001, ****P < 0.0001 (mean with* SD*) (n = 20).*

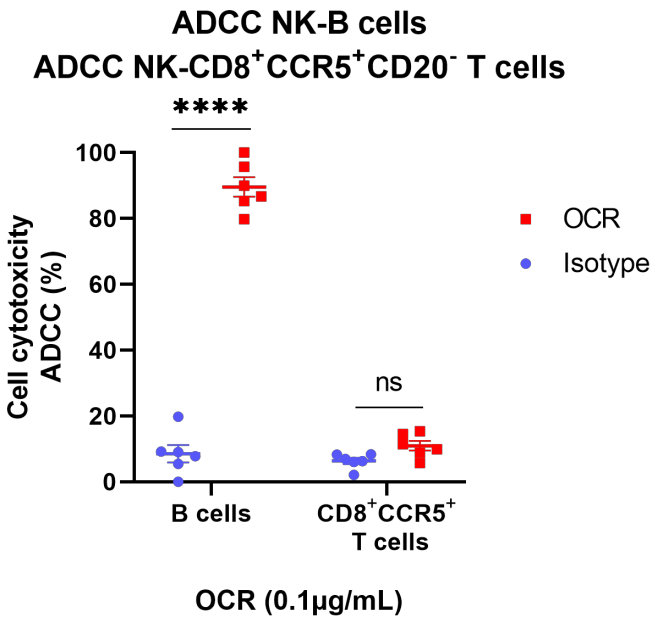

eFigure 6. NK cell cytotoxicity by ADCC against B-cells or $CD8^+CCR5^+CD20^-$ T-cells

CFSE labelled B cells or $CD8^+CCR5^+CD20^-$ T cells were co-cultured with NK cells from 6 healthy donors during 4 hours with Ocrelizumab or control isotype at a concentration of 0.1µg/mL. The effector:target ratio used was 5:1. Cytotoxicity was evaluated by a TO-PRO-3-iodide staining and by flow cytometry analysis. The percentage of cytotoxicity was calculated as: (%TO-PRO-3-$iodide^+CFSE^+$ cells in the co-culture - % TO-PRO-3-$iodide^+CFSE^+$ cells background) / (%TO-PRO-3-$iodide^+CFSE^+$ cells in maximum - % TO-PRO-3-$iodide^+CFSE^+$ cells background) x 100. *Multiple t test was used.* ****$P < 0.0001$; *P=ns (non significant) (mean with SEM) (n = 6).*

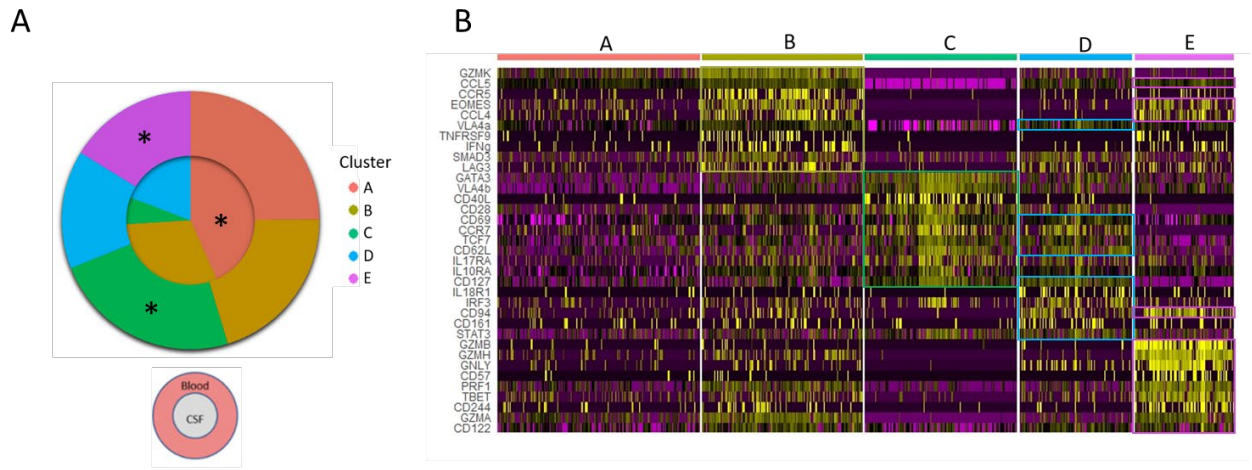

eFigure 7: Identification of CD8^{+}T-cell clusters from blood and CSF samples of patients with other inflammatory neurological diseases.

(A) Pie chart summarizing the cell proportions in each cluster. The inside circle represents cells from CSF, and the outer circle represents cells from the blood. Stars indicate when the proportion in the clusters is significantly higher in one group than the other. **(B)** Heatmap of the most significant genes defining the clusters with the blood and CSF single cells from patients with other inflammatory neurological diseases. Genes that are circled in each cluster are those that are significantly relevant to define the cluster. *Chi2 test was performed to identify significant differences in proportion and adjusted residues were calculated to define these differences between clusters (* mean statistically linked to the group) (A). *P < 0.05, **P < 0.01, ***P < 0.001, ****P < 0.0001 (Blood n=14, CSF n=3)*

Supplementary tables

eTable 1. Listing of antibodies

Panel	Antigen	Fluorochrome	Clone	Manufacturer	Staining Step	Dilution
A. For T-cell profiling						
1-2	Viability	Live/dead blue	-	Thermo Fisher	1st	1:1000
1	CCR7	BV785	G043H7	Biolegend	2nd	1:40
1	CCR5	BV421	2D7/CCR5	BD Biosciences	3rd	1:40
1	CCR6	PE	G034E3	Biolegend	3rd	1:160
1	CD3	BUV395	UCHT1	BD Biosciences	4th	1:40
1	CD8	BUV805	SK1	BD Biosciences	4th	1:160
1	CD4	Alexa 532	RPA-T4	Thermo Fisher	4th	1:80
1	CD19	BV510	HIB19	Biolegend	4th	1:40
1	CD20	BUV737	2H7	BD Biosciences	4th	1:80
1	CD14	FITC	M5E2	Biolegend	4th	1:160
1	CD56	SuperBright600	TULY56	Thermo Fisher	4th	1:40
1	CD16	V450	3G8	BD Biosciences	4th	1:160
1	CD45RA	PercP-Vio700	REA562	Miltenyi biotec	4th	1:400
1	CD161	APC	191B8	Miltenyi biotec	4th	1:100
1	CD49d	PE-Vio770	REA545	Miltenyi biotec	4th	1:400
1	CD11a	PE-Dazzle594	HI111	Biolegend	4th	1:80
1-2	CD3	BUV395	UCHT1	BD Biosciences	2nd	1:40
1-2	CD8	BUV805	SK1	BD Biosciences	2nd	1:160
1-2	CD4	Alexa 532	RPA-T4	Thermo Fisher	2nd	1:80
2	CD127	APC R700	HIL-7R-M21	BD Biosciences	2nd	1:80
2	CD45RC	FITC	MT2	IQ-products	2nd	1:100
2	CD161	PE-Vio770	191B8	Miltenyi biotec	2nd	1:200
2	CD25	PE	2A3	BD Biosciences	2nd	1:40
2	CD39	BV750	GB11	BD Biosciences	2nd	1:100
2	CD103	BUV661	TU66	BD Biosciences	2nd	1:100
2	Granzyme B	V450	Ber-ACT8	BD Biosciences	3rd	1:50
2	Perforin[a]	PercP Cy5,5	B-D48	Biolegend	3rd	1:50
2	Tbet[a]	BV421	4B10	Biolegend	3rd	1:50
2	FoxP3[a]	PE CF594	206D	Biolegend	3rd	1:50
B. For T-cell sorting						
	Viability	Dapi	-	BD biosciences	2nd	1 :100
	CD3	PE	UCHT1	BD Biosciences	1st	1 :100
	CD8	APC-H7	SK1	BD Biosciences	1st	1 :100
	CD45RA	APC-Vio770	T6D11	Miltenyi Biotec	1st	1 :100
	Vα7.2	FITC	3C10	Biolegend	1st	1 :100
C. For Cytotoxic assay						
	CD3	PE-CF594	OKT3	Biologend	1st	1 :100
	CD8	BV510	SK1	BD Biosciences	1st	1 :100
	CD56	V450	B159	BD Biosciences	1st	1 :50
	CD20	PE	2H7	BD Biosciences	1st	1 :10
	CD45RA	APC	HI100	BD Biosciences	1st	1 :20
	CCR7	PE-Cy7	3D12	BD Biosciences	1st	1 :50
	CCR5	FITC	2D7/CCR5	BD Biosciences	1st	1 :50

[a] Intracellular marker

eTable 2. TaqMan probes references

Genes	References
ALCAM	Hs00977641_m1
BLIMP-1	Hs01068508_m1
CCL20	Hs01011368_m1
CCL3	Hs00234142_m1
CCL4	Hs00237011_m1
CCL5	Hs00982282_m1
CCR5	Hs00152917_m1
CCR6	Hs00171121_m1
CCR7	Hs01013469_m1
CD107a	Hs00931464_m1
CD122	Hs01081697_m1
CD127	Hs00904814_m1
CD161	Hs00935894_m1
CD244	Hs00175568_m1
CD25	Hs00907779_m1
CD27	Hs00386811_m1
CD28	Hs01007422_m1
CD3E	Hs01062241_m1
CD38	Hs01120071_m1
CD4	Hs01058407_m1
CD40L	Hs00163934_m1
CD56	Hs00941833_m1
CD57	Hs00218629_m1
CD58	Hs00156385_m1
CD62L	Hs01053460_m1
CD69	Hs00934033_m1
CD8a	Hs00233520_m1
CD94	Hs00233844_m1
CD95	Hs01106214_m1
CTLA4	Hs03044418_m1
EOMES	Hs00172872_m1
FGL2	Hs00173847_m1
FOXP3	Hs00203958_m1
GM-CSF	Hs00171266_m1
GNLY	Hs00246266_m1
GZMA	Hs00989184_m1
GZMB	Hs00188051_m1
GZMH	Hs00277212_m1
GZMK	Hs00157878_m1
IFNg	Hs00174143_m1
IFNgR1	Hs00988304_m1
IL10	Hs00961622_m1
IL10RA	Hs00155485_m1
IL13	Hs00174379_m1
CD103	Hs00559580_m1
IL12A	Hs00168405_m1
IL15	Hs01003716_m1

KLRG1	Hs00195153_m1
BCL2	Hs00608023_m1
IL17RA	Hs01064648_m1
BCL6	Hs00153368_m1
IL18R1	Hs00977691_m1
IL18RAP	Hs00977695_m1
S1PR1	Hs01922614_s1
IL2	Hs00914135_m1
STAT5	Hs00273500_m1
ICOS	Hs04261471_m1
IL23R	Hs00332759_m1
LCK	Hs00178427_m1
IL26	Hs00218189_m1
ID2	Hs04187239_m1
ID3	Hs00954037_g1
DICAM	Hs00260584_m1
IRF1	Hs00971960_m1
IRF3	Hs01547282_m1
IRF4	Hs01056533_m1
Lag3	Hs00158563_m1
LFA1a	Hs00158218_m1
LFA1b	Hs00164957_m1
MCAM	Hs00174838_m1
PD1	Hs01550088_m1
PDL1	Hs01125301_m1
PRF1	Hs00169473_m1
PSGL1	Hs04276253_m1
PLZF	Hs00957433_m1
RORC	Hs01076112_m1
GATA3	Hs00231122-m1
ZAP70	Hs00896345_m1
SMAD3	Hs00969210_m1
STAT3	Hs00374280_m1
TBET	Hs00203436_m1
TCF7	Hs00175273_m1
TGFb1	Hs00171257_m1
TGFbR1	Hs00610320_m1
TGFbR2	Hs00234253_m1
TGFbR3	Hs00234259_m1
TNF	Hs99999043_m1
TNFRSF9	Hs00155512_m1
TNFRSF18	Hs00188346_m1
VLA4a	Hs00168433_m1
VLA4b	Hs01127543_m1
ITGB7	Hs01565750_m1
MYO5A	Hs00165309_m1
HPRT	Hs99999909_m1
TGM2	Hs00190278_m1
B-ACT	Hs99999903_m1

eTable 3. Phenotype of $CD4^+$ and $CD8^+$ T cell clusters

Subset	Cluster	Panel 1	Panel 2
CD4+	C1	EM $CCR5^{int}CCR6^-C161^+$	$CD25^+CD39^+FoxP3^+$
	C2	Naive	$CD127^{int}CD45RC^{int}$
	C3	EM $CCR5^+CCR6^-$	$CD127^{int}CD45RC^{high}$
	C4	EM $CCR5^-CCR6^-$	$CD127^{int}CD103^+$
	C5	CM $CD49d^+CCR6^+CD161^+$	$CD127^{lo}CD161^+$
	C6	Naive $CCR6^+$	$CD127^+CD161^+$
	C7	CM $CCR6^+$	$CD161^+$T-$bet^+Perf^+GzB^+$
	C8	CM $CD49d^-CCR5^-CCR6^-$	$CD127^+$
	C9	CM $CD161^+$	
	C10	TEMRA	
	C11	EM $CCR5^+CCR6^+CD161^+$	
	C12	CM $CD49d^-CCR6^+CD161^-$	
	C13	CM $CD49d^-CCR6^+CD161^+$	
	C14	CM $CD49d^+CCR5^-$ $CCR6^-$	
CD8+	C1	EM $CCR5^+CCR6^-$	T-$bet^+Perf^+GzB^+$
	C2	Naive	T-$bet^+CD45RC^{high}Perf^+GzB^+$
	C3	EM $CCR5^-CCR6^-$	T-$bet^+CD161^{int}CD45RC^{lo}Perf^+Gzb^+$
	C4	CM $CCR5^-CCR6^-$	$CD25^{lo}CD127^+CD161^{high}$
	C5	EM $CCR5^-CCR6^+$	$CD127^{lo}CD161^{int}$
	C6	$CD56^+CD16^+$	T-bet^+GzB^+
	C7	EM $CD161^+$	$CD25^{lo}CD127^{lo}CD45RC^{high}$
	C8	TEMRA $CD161^-$	$CD127^{lo}$
	C9	EM $CCR5^+CCR6^+CD161^{high}$	$CD25^+CD127^+CD39^+CD103^+CD45RC^{high}$
	C10	TEMRA $CD161^+$	$CD25^+CD127^+$ $CD103^+$.

EM (Effector Memory: $CD45RA^-CCR7^-$), CM (Central Memory: $CD45RA^-CCR7^+$), TEMRA (terminally differentiated effector memory cells re-expressing CD45RA: $CD45RA^+CCR7^-$), Naïve ($CD45RA^+CCR7^+$) Perf: Perforin, Gzb: Gramzyme B